

Lagrangian acceleration statistics and relative pair dispersion in turbulent channel flow

J.I. Polanco^a, I. Vinkovic^a, N. Stelzenmuller^b, N. Mordant^b, M. Bourgoïn^c

a. Laboratoire de Mécanique des Fluides et d'Acoustique, CNRS UMR 5509, École Centrale de Lyon, Université Claude Bernard Lyon 1, INSA Lyon, 36 av. Guy de Collongue, 69134 Écully

juan-ignacio.polanco@univ-lyon1.fr

ivana.vinkovic@univ-lyon1.fr

b. Laboratoire des Écoulements Géophysiques et Industriels, CNRS UMR 5519, Université Grenoble Alpes, Domaine Universitaire, CS 40700, 38058 Grenoble

nickolas.stelzenmuller@legi.grenoble-inp.fr

nicolas.mordant@univ-grenoble-alpes.fr

c. Laboratoire de Physique, CNRS UMR 5672, ENS de Lyon, 46 allée d'Italie, 69364 Lyon

mickael.bourgoïn@ens-lyon.fr

Résumé :

Les statistiques lagrangiennes d'accélération dans un écoulement de canal turbulent à $Re_\tau = 1440$ sont obtenues à partir du suivi de particules fluides dans l'expérience et par simulation numérique directe (DNS). L'évolution avec la distance à la paroi des corrélations d'accélération le long des trajectoires est analysée. En proche paroi, les corrélations sont fortement influencées par les tourbillons longitudinaux caractéristiques de la turbulence de paroi. Loin des parois, les corrélations tendent vers un comportement isotrope, même si des signes d'anisotropie à petite échelle persistent jusqu'à très près du centre du canal. Ceci est mis en évidence par une corrélation croisée non nulle entre les composantes d'accélération longitudinale et normale aux parois. Un très bon accord est obtenu entre les résultats expérimentaux et de la DNS pour les statistiques lagrangiennes d'accélération. La dispersion relative de paires de particules fluides est également étudiée à partir de la DNS. La séparation quadratique moyenne $R^2(t) = \langle (\mathbf{D}(t) - \mathbf{D}_0)^2 \rangle$, où $\mathbf{D}(t)$ est la séparation instantanée entre deux particules, est analysée à différentes distances de la paroi et pour différentes séparations initiales \mathbf{D}_0 . Dans tous les cas, le comportement aux temps courts est en accord avec le développement limité de R^2 , prédisant au premier ordre le régime balistique où R^2 évolue comme t^2 . À des temps intermédiaires, pour des séparations initiales dans la gamme des échelles inertielles, le régime prédit par RICHARDSON [1] où R^2 évolue comme t^3 est atteint.

Abstract :

Lagrangian statistics of acceleration in a fully-developed turbulent channel flow at $Re_\tau = 1440$ are obtained from tracking of tracer particles in experiments and direct numerical simulations (DNS). The wall-distance dependency of acceleration correlations along particle paths is analysed. Near the channel walls, the correlations are strongly affected by quasi-streamwise vortices characteristic of near-wall turbulence. Further away from the walls, acceleration statistics approach isotropy, although signs of

small-scale anisotropy persist near the channel centre. This is evidenced by a non-zero cross-correlation between the streamwise and wall-normal acceleration components at nearly all wall distances. Very good agreement between the experimental results and the DNS is achieved for the Lagrangian acceleration statistics. Relative dispersion of tracer particle pairs is also studied by DNS. The mean square separation $R^2(t) = \langle (\mathbf{D}(t) - \mathbf{D}_0)^2 \rangle$, where $\mathbf{D}(t)$ is the instantaneous separation of a particle pair, is analysed at different wall distances and for different initial separations \mathbf{D}_0 . In all cases, the short-time behaviour is consistent with the Taylor expansion of R^2 , which predicts a ballistic regime where R^2 grows as t^2 at the leading order. At later times, for initial separations in the inertial range, the regime predicted by Richardson [1] in which the evolution of R^2 scales with t^3 is approached.

Mots clefs : turbulence inhomogène, turbulence lagrangienne, accélération, dispersion de paires

1 Introduction

In the Lagrangian framework, a flow is described from the viewpoint of passive tracers moving with the fluid velocity field. This approach is particularly well suited for the study of dispersion phenomena such as the transport of pollutants in atmospheric flows. It has been often used to describe turbulent flows in experiments and by direct numerical simulations [2].

The Lagrangian description of turbulence is the basis of a number of stochastic models attempting to predict the motion of passive tracers advected by turbulent flows. These models are typically based on a Langevin equation describing the temporal increment of tracer velocity in terms of the Lagrangian integral time scale [3]. Higher-order models such as proposed by Sawford [4] take into account finite Reynolds number effects by including time scales associated to the Lagrangian acceleration of the fluid flow, which is related to the smallest scales of turbulent motion.

The statistical description of the relative dispersion between a pair of tracer particles can be applied to understand the evolution of a particle cloud within a turbulent flow. The study of particle pair dispersion in statistically isotropic turbulent flows was pioneered by Richardson [1] and was further developed by Obukhov and Batchelor [5–7]. They concluded that the mean square separation of particle pairs with initial separation \mathbf{D}_0 in the inertial range ($\eta \ll D_0 \ll L$, where η and L represent the smallest and largest scales of turbulent motion respectively) initially follows a ballistic regime

$$R^2(t) \equiv \langle (\mathbf{D}(t) - \mathbf{D}_0)^2 \rangle = \langle \delta \mathbf{v}_0^2 \rangle t^2 \quad \text{for } t \ll t_0, \quad (1)$$

where the characteristic time scale t_0 depends on the initial separation $D_0 = |\mathbf{D}_0|$. Here $\mathbf{D}(t)$ is the instantaneous separation of a particle pair and $\delta \mathbf{v}_0$ is their initial relative velocity. The above expression is purely kinematic, and can be readily deduced from the short-time Taylor expansion of $\mathbf{D}(t)$.

From dimensional arguments following Kolmogorov's (K41) theory [8], Obukhov [5] determined that at intermediate times the relative dispersion process only depends on the mean turbulent energy dissipation ε and time t . Thus the mean square separation of pairs takes the form

$$R^2(t) = g\varepsilon t^3 \quad \text{for } t_0 \ll t \ll T_L, \quad (2)$$

where T_L is the Lagrangian integral time scale and g is the so-called Richardson constant, supposed universal.

Most existent Lagrangian investigations of turbulence have attempted to describe homogeneous isotropic turbulent flows. However, realistic flows are generally not isotropic nor homogeneous due to the presence of features such as solid obstacles and boundaries. In this work we aim at describing a wall-bounded turbulent flow from a Lagrangian viewpoint. Wall-bounded turbulence is characterised by strong average shear in the vicinity of the walls. Moreover, the fluctuating flow is dominated by the presence of elongated quasi-streamwise vortices near the walls and other coherent motions spanning a wide range of scales [9]. This results in a flow that is strongly anisotropic, especially in the near-wall region.

Results from experiments and direct numerical simulations (DNS) of a turbulent channel flow at the same friction Reynolds number $Re_\tau = 1440$ are presented, with an emphasis on Lagrangian acceleration statistics across the channel. Moreover, relative pair dispersion statistics obtained from channel flow DNS are presented and compared with the theoretical predictions for homogeneous isotropic turbulence (HIT). In Section 2, the experimental and numerical set-ups are briefly introduced. In Section 3, Lagrangian acceleration statistics from experiments and DNS are presented. This is followed by particle pair dispersion statistics from DNS in Section 4. Finally, Section 5 presents the main conclusions of this work.

2 Experiments and DNS

Experiments and numerical simulations are performed to study a turbulent channel flow between two parallel walls separated by a distance $2h$. The Reynolds number based on the mean velocity U_0 at the channel centre is $Re = U_0 h / \nu = 34\,000$, where ν is the kinematic viscosity. This corresponds to a friction Reynolds number $Re_\tau = u_\tau h / \nu = 1440$, where $u_\tau = \sqrt{\tau_w / \rho}$ is the friction velocity associated to the wall shear stress τ_w . In the following, the subscript $+$ is used to indicate physical quantities non-dimensionalised by u_τ and ν .

2.1 Experiments

The experiment is performed in a closed-loop water tunnel. Measurements are made in a test section with a rectangular cross-section of dimensions $37.5 \times 316 \text{ mm}^2$ and a mean centreline velocity $U_0 = 1.75 \text{ m/s}$. The flow is seeded with neutrally-buoyant spherical particles of diameter $10 \mu\text{m}$, which is small enough to accurately trace the flow down to the viscous layer. Three-dimensional particle trajectories are measured by particle tracking velocimetry in a $35 \times 20 \times 8 \text{ mm}^3$ measurement volume illuminated by a 8 mm-thick laser sheet using two high-speed cameras with a sampling rate of 25 000 frames/s. Particle velocity and acceleration are obtained by convolution of the trajectories with Gaussian differentiating kernels, which also filter out noise from the measurements [10]. This experimental set-up enables the accurate detection of particles for wall distances in the interval $y^+ \in [4, 1400]$, that is, in nearly one half of the channel. The detection of particles very near the wall presented difficulties related to reflexion of images on the wall.

2.2 DNS

For the numerical simulations, a pseudo-spectral method [11] is used to solve the Navier-Stokes equations between two parallel walls. The solver is coupled with Lagrangian tracking of tracer particles. The numerical domain is periodic in the streamwise (x) and spanwise (z) directions, where the solution is

decomposed into Fourier modes. In the wall-normal (y) direction, a Chebyshev expansion is applied and no-slip boundary conditions are enforced. The domain size is $L_x \times L_y \times L_z = 4\pi h \times 2h \times \pi h$, and the velocity field is decomposed into $2048 \times 433 \times 1024$ spectral modes. The acceleration field is obtained in the Eulerian frame from the resolved velocity \mathbf{u} according to $\mathbf{a} = \partial\mathbf{u}/\partial t + \nabla(\mathbf{u}^2/2) + (\nabla \times \mathbf{u}) \times \mathbf{u}$. The velocity and acceleration fields are then interpolated at each particle position using third-order Hermite polynomials. The presented acceleration statistics from DNS correspond to a first simulation in which 2×10^6 tracer particles were initialised at random positions in the domain.

A second numerical simulation is performed to study pair dispersion statistics. In this case, tracers are initialised at chosen locations in order to characterise the influence of both the initial position of each pair in the channel, and of their relative initial separation \mathbf{D}_0 . A total of 10 initial wall distances y_0^+ ranging from 3 to 1440 are chosen. At each wall distance, particle pairs are given initial separations $D_0/\eta = 1, 4, 16, 32$ and 64 . Moreover, for each initial separation, particle pairs are oriented in each of the 3 Cartesian directions x, y and z in order to study the effect of anisotropy. This results in 150 different parameter combinations. For each combination, the size of the statistical sample (i.e. the number of particle pairs) is about 20 000.

3 Acceleration statistics

3.1 Mean and variance profiles

Experimental and DNS mean and variance acceleration profiles across the channel are presented in Figure 1. The results from both approaches are compared with those of Yeo et al. [12], who analysed Eulerian acceleration statistics from DNS of turbulent channel flow at a lower Reynolds number, $Re_\tau = 600$. The three sets of results are mostly consistent. Departure and increased uncertainty are observed for the experimental data in the near-wall region, which can be associated to the difficulties of detecting particles very near the walls. The mean streamwise acceleration is found to be negative near the wall, which is associated to increasing viscous effects in that region, while the positive wall-normal acceleration corresponds to an increased contribution of the average wall-normal pressure gradient [12].

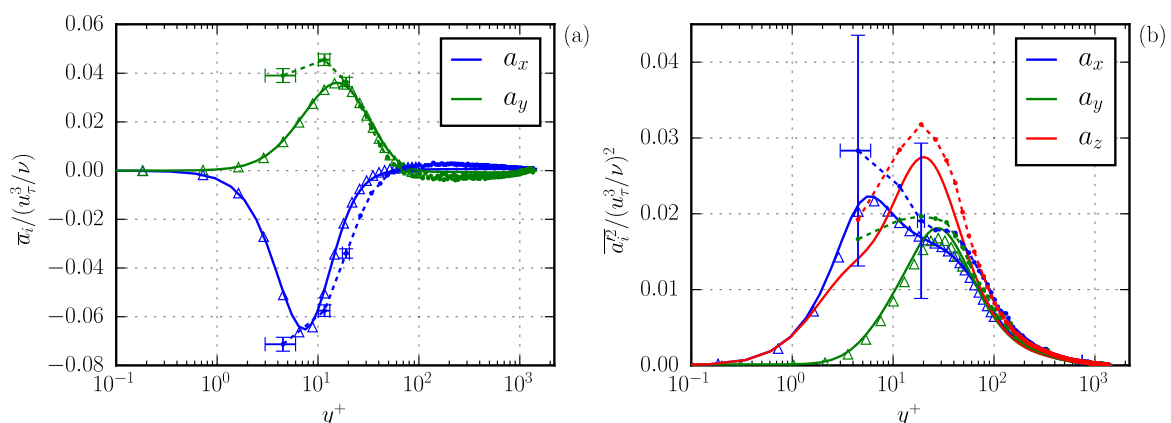


Figure 1 – Mean and variance acceleration profiles across the channel. Comparison between experiments (dashed lines), DNS (solid lines) and Yeo et al. [12] DNS at $Re_\tau = 600$ (triangles).

The acceleration variance profiles in Figure 1(b) indicate that the largest acceleration fluctuations occur near the walls. In that region, the standard deviation of the fluctuations is considerably larger than the magnitude of the mean acceleration components, implying that the fluctuating acceleration plays an

important role in the near-wall dynamics. As shown by Lee et al. [13], the acceleration dynamics near the wall are dominated by the presence of quasi-streamwise vortices, which induce high-magnitude centripetal accelerations towards their centres of rotation. This effect is responsible for most of the acceleration fluctuations in the wall-normal and spanwise directions in that region.

3.2 Lagrangian correlations

The Lagrangian approach describes the temporal evolution of a physical quantity along the trajectory of tracer particles. Lagrangian statistics are then parametrised by the initial position \mathbf{r}_0 of the considered trajectories at a time t_0 and by a time delay τ relative to t_0 . In the case of a statistically stationary flow, statistics do not depend on t_0 itself but do depend on τ . Moreover, the statistical homogeneity of a turbulent channel flow in the streamwise and spanwise directions implies that dependency on initial position \mathbf{r}_0 reduces to a dependency on the initial wall distance y_0 . In conclusion, Lagrangian statistics depend on y_0 and τ . Acceleration correlations presented further below are obtained after the Lagrangian averaging procedure. The result of applying the Lagrangian averaging procedure to particle positions is presented in Figure 2 for illustration.

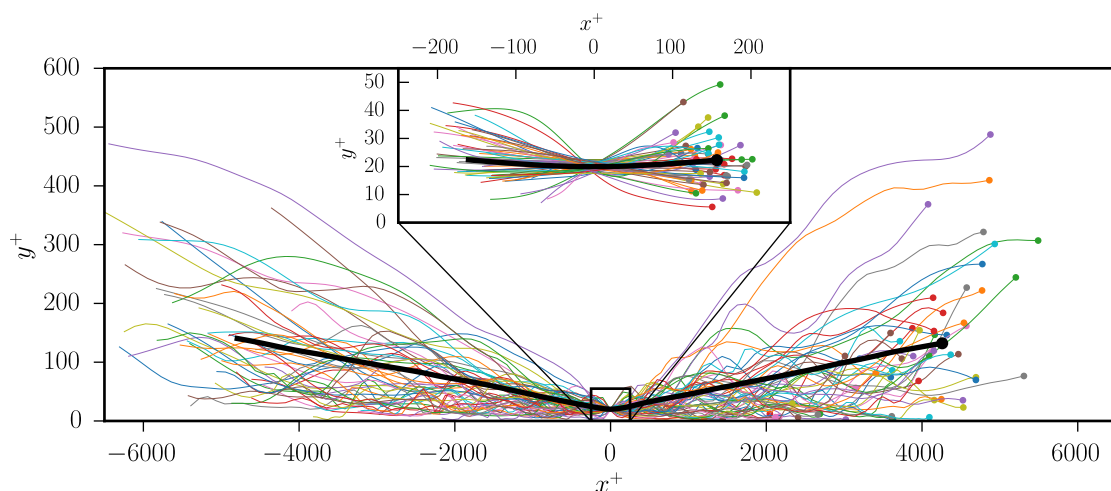


Figure 2 – Illustration of the Lagrangian averaging procedure. Thin curves represent trajectories of particles located at $y_0^+ = 20 \pm 2.5$ at a reference time t_0 . The thick curve represents the Lagrangian average of particle position $\langle \mathbf{r}(\tau, y_0) \rangle$. For illustration purposes, trajectories are shifted in x so that $x(t_0) = 0$.

Lagrangian time scales and coupling between acceleration components can be deduced from the Lagrangian acceleration correlation tensor, defined as

$$\rho_{ij}(\tau, y_0) = \frac{\langle a'_i(t_0, y_0) a'_j(t_0 + \tau, y_0) \rangle}{\langle a_i'^2(t_0, y_0) \rangle^{1/2} \langle a_j'^2(t_0 + \tau, y_0) \rangle^{1/2}}, \quad (3)$$

where $a'_i(t_0 + \tau, y_0) = a_i(t_0 + \tau, y_0) - \langle a_i(t_0 + \tau, y_0) \rangle$ is the fluctuation of fluid particle acceleration relative to its Lagrangian average, and $i = x, y$ or z . This estimator thus quantifies the correlation between the a_i component at an initial time, and the a_j component after a time lag τ , along trajectories of fluid particles initially located at y_0 .

Figure 3 shows the Lagrangian auto-correlation of the three acceleration components for different initial wall distances y_0 . Correlations are presented for positive and negative time delays τ . The curves show

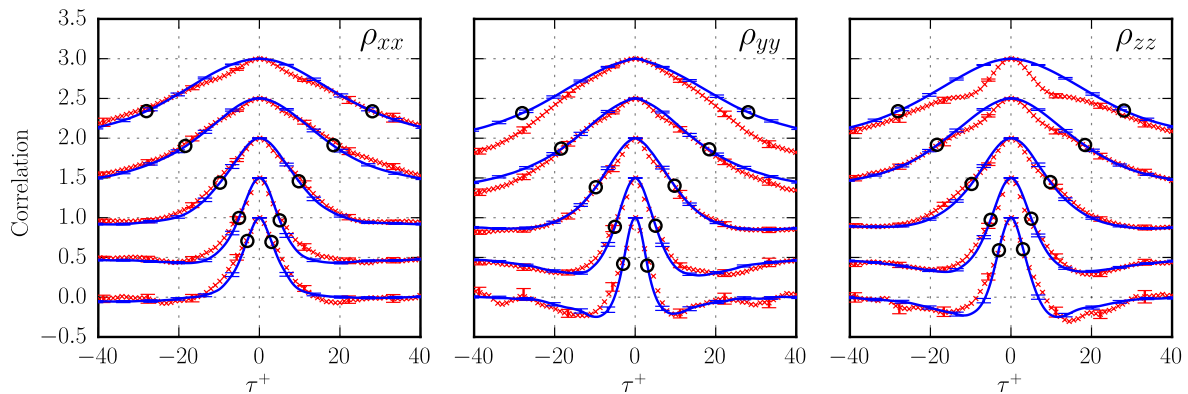


Figure 3 – Lagrangian auto-correlations of streamwise (ρ_{xx}), wall-normal (ρ_{yy}) and spanwise (ρ_{zz}) fluid particle acceleration from experiments (crosses) and DNS (lines). Circles indicate time lags $\tau = \pm\tau_\eta$. Error bars indicate the 95% confidence interval. Curves are shifted vertically by increments of 0.5 for clarity. From bottom to top, the curves correspond to particles located initially at $y_0^+ = 20, 60, 200, 600$ and 1000. (The channel centre is at $y^+ = 1440$.)

a good agreement between experiments and DNS. The shown auto-correlations are rather symmetric in time, e.g. $\rho_{xx}(\tau, y_0) \approx \rho_{xx}(-\tau, y_0)$. The flow inhomogeneity is clearly visible in the fact that the decorrelation time of all acceleration components increases with y_0 . This decorrelation time τ_0 has the same order of magnitude as local Kolmogorov time scale $\tau_\eta(y_0)$ (represented by black circles), which increases with wall distance. For instance, at $y_0^+ = 200$, the three auto-correlations ρ_{xx} , ρ_{yy} and ρ_{zz} cross zero at $|\tau_0^+| \approx 20$, while $\tau_\eta^+ \approx 9.8$ at that wall distance. In general, it is found that $|\tau_0| \approx 2\tau_\eta$ far from the walls, which is consistent with results in HIT [14].

As expected, anisotropy is mainly visible for small wall distances. Near the wall ($y^+ = 20$), the streamwise acceleration stays correlated for far longer than the other two components. The latter become negative after $\tau \approx 2\tau_\eta$ (similarly to HIT), indicating that there is a tendency for a'_y and a'_z to change sign after $2\tau_\eta$. Near the walls, these two components are strongly affected by the presence of streamwise vortices. A fluid particle trapped in one such vortex experiences strong centripetal accelerations towards the vortex rotation axis [13], which can help explain the negative ρ_{yy} and ρ_{zz} correlations. This behaviour is not limited to wall-bounded turbulent flows, however. In HIT, it has been observed that fluid particles experience similar high-acceleration events in the vicinity of vortex filaments, and the auto-correlation of the centripetal component of these accelerations become negative to a much greater degree than the auto-correlation of the component parallel to the vortex filament [15, 16].

In Figure 4(a), the Lagrangian auto-correlation of acceleration magnitude $|\mathbf{a}|$ is shown. The decorrelation time of $|\mathbf{a}|$ is considerably larger than that of the components. That is, changes in the orientation of the acceleration vector are much more sudden than changes in its magnitude. This is again consistent with observations in HIT [14, 17]. In Figures 4(b) and (c), the cross-correlations ρ_{xy} and ρ_{yz} are presented. The latter is zero at all wall distances owing to the statistical symmetry $z \leftrightarrow -z$ in the channel. As for ρ_{xy} , it is non-zero at all the considered wall distances. Moreover, it is asymmetric in time, tending to an antisymmetric behaviour ($\rho_{xy}(\tau, y_0) \approx -\rho_{xy}(-\tau, y_0)$) far from the walls. The correlation peak is always found after a small time delay $|\tau|/\tau_\eta \approx 0.6$.

The time asymmetry and the small time scale of variation of ρ_{xy} are evidences of the existence of small-scale anisotropy even far from the walls, where turbulence may be expected to approach an isotropic state. The curves imply that, in general, a positive acceleration a'_x is followed by a negative acceleration

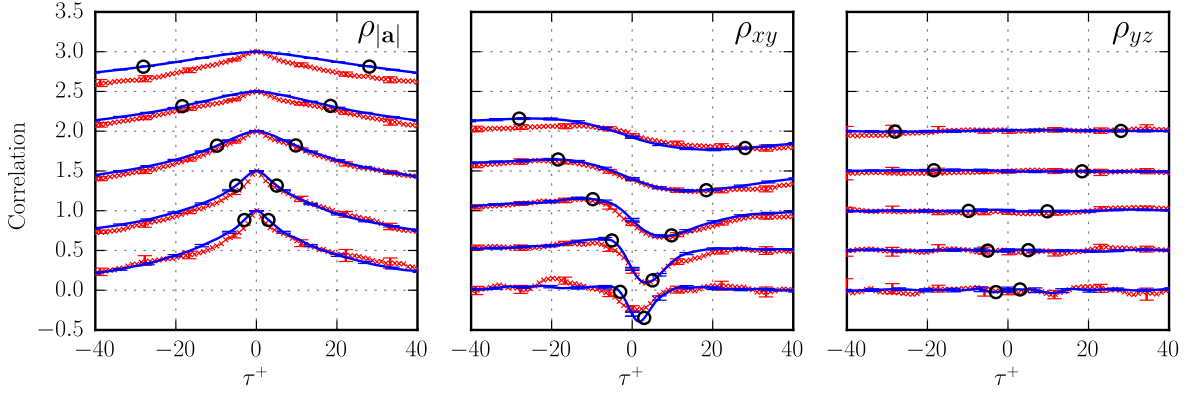


Figure 4 – Lagrangian auto-correlation of acceleration magnitude ($\rho_{|a|}$), and cross-correlations between acceleration components ρ_{xy} and ρ_{yz} . (For details, see Fig. 3).

a'_y after a small time delay, or vice versa. This suggests that there is a preferential direction of rotation of the acceleration fluctuation vector \mathbf{a}' projected on the x - y plane. This preferential direction of rotation is consistent with the direction of the mean shear, or equivalently with the sign of the corresponding mean vorticity $\bar{\omega}_z = -d\bar{u}/dy$, which is negative in the lower half of the channel where the presented statistics are obtained.

4 Particle pairs

The relative dispersion of pairs of fluid particles can be described by the mean square change of separation $R^2(t) = \langle (\mathbf{D}(t) - \mathbf{D}_0)^2 \rangle$, where $\mathbf{D}(t)$ is the instantaneous separation of a pair of particles and $\mathbf{D}_0 = \mathbf{D}(0)$. At very short times, the evolution of the pair separation can be expressed as $\mathbf{D}(t) = \mathbf{D}_0 + \delta\mathbf{v}_0 t + \frac{1}{2}\delta\mathbf{a}_0 t^2 + \mathcal{O}(t^3)$, where $\delta\mathbf{v}_0$ and $\delta\mathbf{a}_0$ are the relative velocity and acceleration of the pair. This leads to

$$R^2(t) = \langle \delta\mathbf{v}_0^2 \rangle t^2 + \langle \delta\mathbf{v}_0 \cdot \delta\mathbf{a}_0 \rangle t^3 + \mathcal{O}(t^4) \quad \text{for } t \ll t_0. \quad (4)$$

Note that this is a purely kinematic relation and does not take into account the effects of turbulence on the dispersion process. The characteristic time t_0 can be interpreted as the memory of the initial condition before turbulent dispersion effects take place. In the following, it is estimated as $t_0 = D_0^{2/3} \varepsilon^{-1/3}$. This definition was introduced by Batchelor [6] to estimate the duration of the short-time dispersion regime, assuming that the initial separation lies in the inertial range ($\eta \ll D_0 \ll L$), and corresponds to the eddy-turnover time at scale D_0 [18].

At the leading order, R^2 follows a ballistic regime which depends on the second-order Eulerian velocity structure function $S_2(\mathbf{r}_0, \mathbf{D}_0) = \overline{[\mathbf{u}(\mathbf{r}_0 + \mathbf{D}_0) - \mathbf{u}(\mathbf{r}_0)]^2} = \langle \delta\mathbf{v}_0^2 \rangle$, where \mathbf{r}_0 is the initial position of one of the particles in a pair. At the next order, the t^3 term is governed by the crossed velocity-acceleration structure function $\langle \delta\mathbf{v}_0 \cdot \delta\mathbf{a}_0 \rangle$, which is equal to -2ε in stationary HIT [19, 20]. The negative sign of this coefficient indicates that the initial ballistic regime should be followed by a deceleration of the dispersion process when going forwards in time for $t \ll t_0$. Its negative sign has also been linked to the temporal asymmetry of turbulence, since it implies that, at short times, a pair of particles separates faster backwards in time (i.e. for $t < 0$) than forwards ($t > 0$) [21].

The initial spatial configuration of a pair of particles can be described in terms of the initial position of one of the particles, \mathbf{r}_0 , and the initial separation vector between the two particles, \mathbf{D}_0 , so that the second

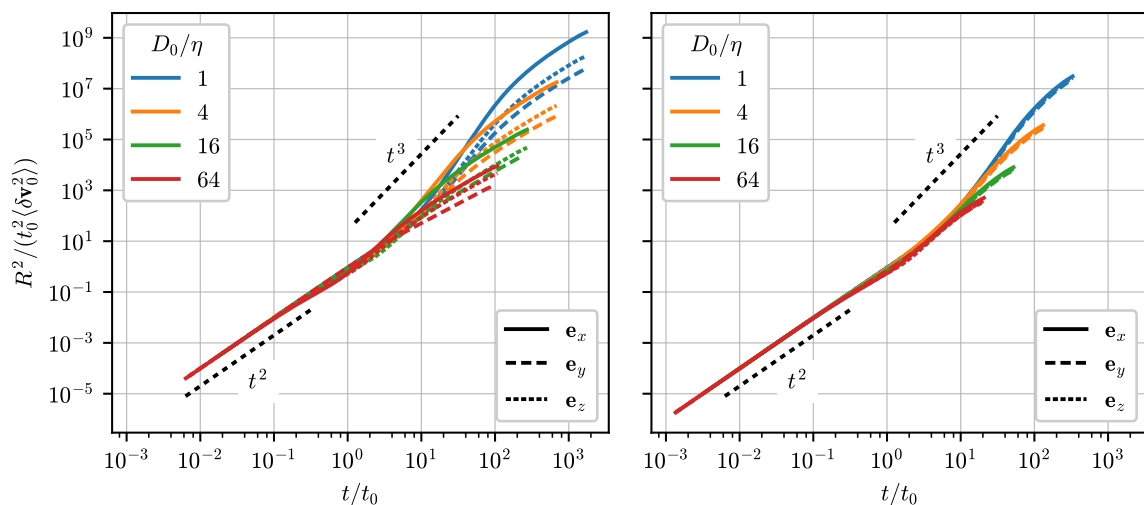


Figure 5 – Time evolution of the mean square separation, compensated by the second-order structure function $\langle \delta \mathbf{v}_0^2 \rangle = S_2(y_0, \mathbf{D}_0)$ and the eddy-turnover time $t_0 = D_0^{2/3} \varepsilon^{-1/3}$. Pairs are initially located at $y_0^+ = 18$ (left) and 427 (right). Colours represent different initial separations D_0 . Line styles represent different initial orientations.

particle is initially located at $\mathbf{r}_0 + \mathbf{D}_0$. In a statistically stationary flow, Lagrangian relative dispersion statistics depend both on \mathbf{r}_0 and \mathbf{D}_0 , in addition to the time t relative to the initial time. As with the Lagrangian statistics described in Section 3.2, the dependency on \mathbf{r}_0 can be reduced to a dependency on y_0 in channel flow, where y_0 is the wall-normal component of \mathbf{r}_0 .

In Figure 5, the time evolution of the mean square separation $R^2(t)$ is shown for groups of particle pairs at two initial wall distances, $y_0^+ = 18$ and 427. For each wall-normal distance, the results obtained for 12 initial separations $\mathbf{D}_0 = D_0 \mathbf{e}_0$ are presented. Here \mathbf{e}_0 is a unitary vector indicating the initial orientation of a pair of particles, and is chosen as a vector in the Cartesian basis $\{\mathbf{e}_x, \mathbf{e}_y, \mathbf{e}_z\}$. In all cases, the ballistic regime $R^2 \approx \langle \delta \mathbf{v}_0^2 \rangle t^2$ is observed at the shortest times. As expected, the effect of the initial orientation is most important near the wall. Using the proposed scaling, the separation of particles initially oriented in the streamwise direction is larger than that of the other orientations. This is due to the scaling itself. It can be explained by the differences in the Eulerian velocity structure function $S_2(\mathbf{r}_0, \mathbf{D}_0)$, which in wall-bounded flows depends both on the magnitude and on the orientation of \mathbf{D}_0 , in addition to the initial wall distance y_0 . In the near-wall region, for a fixed separation $D_0 = |\mathbf{D}_0|$ in the inertial range, S_2 is smaller in the streamwise direction since the Eulerian velocity field is most correlated in that direction.

In general, at intermediate times, an acceleration of the dispersion process is observed, which is qualitatively consistent with Richardson's predictions. However, from the presented curves it is not clear whether Richardson's t^3 regime is found. It does seem that, for the smallest separation $D_0/\eta = 1$ (which is not really within the inertial range), the mean square separation undergoes a regime where it grows faster than t^3 .

The mean square separation scaled against the ballistic regime $\langle \delta \mathbf{v}_0^2 \rangle t^2$ is plotted on Figure 6. The ballistic regime scaling works for times smaller than $t/t_0 \approx 0.1$. In all cases, the ballistic regime is followed by a transient deceleration of the diffusion process, which is likely related to the sign of $\langle \delta \mathbf{v}_0 \cdot \delta \mathbf{a}_0 \rangle$ in the t^3 term of equation (4). Presumably, this term is negative and becomes important at that stage. This transient state is followed by a highly diffusive regime that might be assimilated to Richardson's

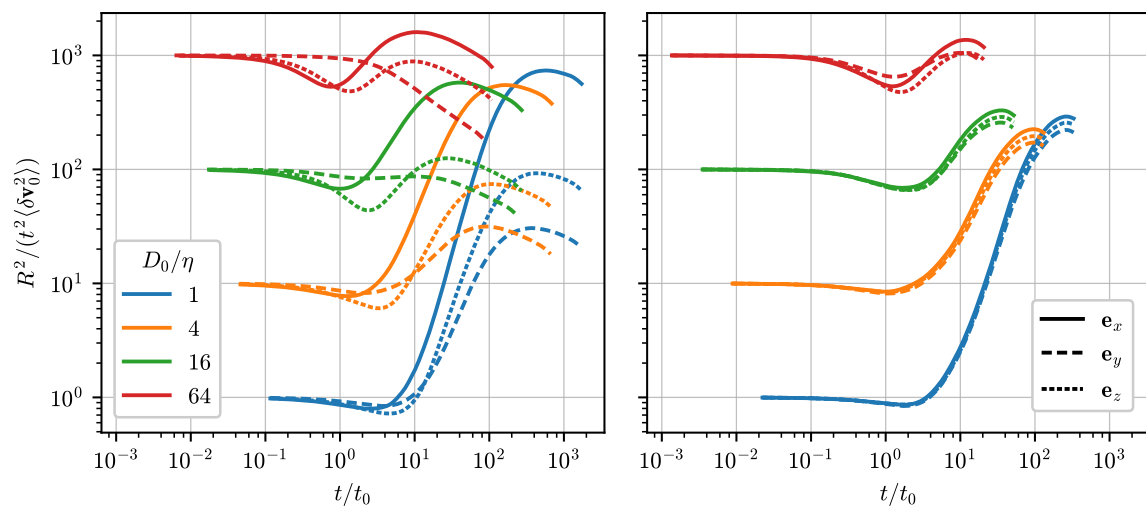


Figure 6 – Time evolution of the mean square separation, compensated by the ballistic regime $\langle \delta \mathbf{v}_0^2 \rangle t^2$. Pairs are initially located at $y_0^+ = 18$ (left) and 427 (right). Curves are shifted vertically by steps of one decade for clarity.

prediction. This regime ends with a plateau at long times. The available data suggest that this is followed by a deceleration of the dispersion process. At very long times, the motion of particles in a pair can be expected to become completely decorrelated. In that case, the mean square separation of pairs would follow a normally-diffusive regime represented by a linear evolution of R^2 .

5 Conclusions

The inhomogeneous turbulent flow in a plane channel is described in terms of Lagrangian statistics of acceleration obtained from experiments and direct numerical simulations at the same Reynolds number. The phenomenology of near-wall turbulence is shown to have a clear signature on the acceleration of tracer particles, which is strongly affected by the presence of near-wall coherent structures as seen in the Lagrangian auto-correlations of acceleration components. Moreover, Lagrangian cross-correlations between the streamwise and wall-normal acceleration components infer the existence of small-scale anisotropy in the bulk of the channel. These results can serve as basis for the determination of time scales intrinsic to inhomogeneous (or wall-bounded) turbulence, which can in turn contribute to the improvement of stochastic models for such flows [22].

In a second part, pair dispersion statistics from direct numerical simulations in a turbulent channel flow are analysed. Some of the classical scalings of the dispersion process are recovered [1, 6]. The initial ballistic regime, in which the mean square separation of pairs $R^2(t)$ grows as $\langle \delta \mathbf{v}_0^2 \rangle t^2$, is clearly captured. This regime is followed by a transient deceleration of the separation process, still at short times, which is qualitatively consistent with the expectation of a negative $\langle \delta \mathbf{v}_0 \cdot \delta \mathbf{a}_0 \rangle t^3$ term in the Taylor expansion of $R^2(t)$, and which has been associated to the irreversibility of turbulence [21]. At intermediate times, the mean square separation of pairs grows faster than the ballistic regime, which again is qualitatively consistent with Richardson's prediction. However, many questions remain to be answered. The mentioned qualitative agreements must yet be verified from available numerical data in order to characterise the actual quantitative agreement with the expected results. Moreover, it is not clear from the presented

results whether the chosen characteristic time scale $t_0 = D_0^{2/3} \varepsilon^{-1/3}$ is the most appropriate to describe the short-time dispersion process. Finally, the effect of inhomogeneity and anisotropy on pair separation, as well as the effect of the mean flow, remain to be quantified.

References

- [1] L. F. Richardson. « Atmospheric Diffusion Shown on a Distance-Neighbour Graph ». *Proc. R. Soc. Lond. Ser. A* 110.756 (1926), pp. 709–737.
- [2] F. Toschi and E. Bodenschatz. « Lagrangian Properties of Particles in Turbulence ». *Annu. Rev. Fluid Mech.* 41.1 (2009), pp. 375–404.
- [3] S. B. Pope. « Lagrangian PDF methods for turbulent flows ». *Ann. Rev. Fluid Mech.* 26 (1994).
- [4] B. L. Sawford. « Reynolds number effects in Lagrangian stochastic models of turbulent dispersion ». *Phys. Fluids A* 3.6 (1991), pp. 1577–1586.
- [5] A. M. Obukhov. « On the distribution of energy in the spectrum of turbulent flow ». *Izv. Akad. Nauk SSSR* 5 (1941), pp. 453–66.
- [6] G. K. Batchelor. « The application of the similarity theory of turbulence to atmospheric diffusion ». *Q.J.R. Meteorol. Soc.* 76.328 (1950), pp. 133–146.
- [7] J. P. L. C. Salazar and L. R. Collins. « Two-Particle Dispersion in Isotropic Turbulent Flows ». *Annu. Rev. Fluid. Mech.* 41.1 (2009), pp. 405–432.
- [8] A. N. Kolmogorov. « The Local Structure of Turbulence in Incompressible Viscous Fluid for Very Large Reynolds Numbers ». *Dokl. Akad. Nauk SSSR* 30 (1941), pp. 301–305.
- [9] A. J. Smits, B. J. McKeon and I. Marusic. « High-Reynolds Number Wall Turbulence ». *Annu. Rev. Fluid Mech.* 43.1 (2011), pp. 353–375.
- [10] N. Mordant, A. M. Crawford and E. Bodenschatz. « Experimental Lagrangian acceleration probability density function measurement ». *Physica D* 193.1–4 (2004), pp. 245–251.
- [11] M. Buffat, L. Le Penven and A. Cadiou. « An efficient spectral method based on an orthogonal decomposition of the velocity for transition analysis in wall bounded flow ». *Comput. Fluids* 42.1 (2011), pp. 62–72.
- [12] K. Yeo, B.-G. Kim and C. Lee. « On the near-wall characteristics of acceleration in turbulence ». *J. Fluid Mech.* 659 (2010), pp. 405–419.
- [13] C. Lee, K. Yeo and J.-I. Choi. « Intermittent Nature of Acceleration in Near Wall Turbulence ». *Phys. Rev. Lett.* 92.14 (2004), p. 144502.
- [14] P. K. Yeung and S. B. Pope. « Lagrangian statistics from direct numerical simulations of isotropic turbulence ». *J. Fluid Mech.* 207 (1989), pp. 531–586.
- [15] N. Mordant, E. Lévêque and J.-F. Pinton. « Experimental and numerical study of the Lagrangian dynamics of high Reynolds turbulence ». *New J. Phys.* 6 (2004), pp. 116–116.
- [16] F. Toschi, L. Biferale, G. Boffetta, A. Celani, B. J. Devenish and A. Lanotte. « Acceleration and vortex filaments in turbulence ». *J. Turbulence* 6 (2005), N15.
- [17] N. Mordant, A. M. Crawford and E. Bodenschatz. « Three-Dimensional Structure of the Lagrangian Acceleration in Turbulent Flows ». *Phys. Rev. Lett.* 93.21 (2004), p. 214501.

- [18] U. Frisch. *Turbulence: The Legacy of A. N. Kolmogorov*. Cambridge University Press, 1995.
- [19] J. Mann, S. Ott and J. S. Andersen. *Experimental study of relative, turbulent diffusion*. Tech. rep. Risø-R-1036(EN). Roskilde, Denmark: Risø National Laboratory, 1999.
- [20] R. J. Hill. « Opportunities for use of exact statistical equations ». *J. Turbul.* 7 (2006), N43.
- [21] J. Jucha, H. Xu, A. Pumir and E. Bodenschatz. « Time-reversal-symmetry breaking in turbulence ». *Phys. Rev. Lett.* 113.5 (2014).
- [22] S. B. Pope. « Stochastic Lagrangian models of velocity in homogeneous turbulent shear flow ». *Phys. Fluids* 14.5 (2002), pp. 1696–1702.